

ARSENIC REMOVAL FROM GEOTHERMAL BORE WATER: THE EFFECT OF DISSOLVED SILICA

P.J. SWEDLUND¹, J.G. WEBSTER¹ AND G.M. MISKELLY²

¹ ESR Environmental, Auckland, NZ

² Department of Chemistry, The University of Auckland, NZ

SUMMARY - Arsenic adsorption onto a hydrous ferric oxide (HFO) floc is a viable option for the removal of arsenic (**As**) from geothermal bore waters. However, the degree of **As(III)** and **As(V)** adsorption from bore water is considerably less than that from a 0.1M NaNO₃ electrolyte, or than that predicted using equilibrium surface complexation constants and the geochemical speciation model, MINTEQA2. By determining the effect of individual bore water components on the adsorption of **As(III)** and **As(V)** from 0.1M NaNO₃, mono-silicic acid (H₄SiO₄) was identified as the main component inhibiting **As** adsorption. Mono-silicic acid is adsorbed onto the HFO surface when the H₄SiO₄/Fe ratio of the solid is below ca. 0.2, and polymerised on the surface at higher H₄SiO₄/Fe ratios. Both of these processes appear to inhibit **As** adsorption from bore water. By altering the MINTEQA2 data base to include a surface complexation constant for H₄SiO₄ adsorption onto HFO, prediction accuracy is improved. However, MINTEQA2 continues to overestimate the degree of **As(III)** adsorption, and of **As(V)** adsorption at pH > 8. This is considered to reflect the effect of H₄SiO₄ polymerisation on the HFO surface, a process which is not taken into account by the speciation model.

1.0 INTRODUCTION

In 1993 the World Health Organisation (WHO) decreased the guideline for arsenic (**As**) in drinking water from 50 µg L⁻¹ to a provisional value of 10 µg L⁻¹ (WHO 1993). Arsenic concentrations in New Zealand's Waikato River typically vary between 10 and 80 µg L⁻¹ and several drinking water supplies that derive water from this river border on, or exceed, the revised **As** guideline (Davies et al. 1994). The largest source of **As** entering the Waikato River is the Wairakei Geothermal Power Station's discharge of spent bore water containing approximately 4,000 µg L⁻¹ **As** (Aggett and Aspell 1978). Discharge options that avoid or mitigate this **As** contamination are currently being investigated.

Flocculation with HFO is an effective treatment process for the adsorptive removal of **As** from waste water, although the efficiency of **As** adsorption is dependent on variables such as pH and **As** oxidation state (Peng and Di 1994). For example, in oxygen-rich waters the predominant **As** species are the **As(V)** oxy-anions of arsenic acid (H₃AsO₄; pK_{a1, 2 & 3} = 2.2, 6.9 and 11.5 respectively), which adsorb most efficiently at low pH. In oxygen-deficient waters, such as fresh geothermal bore water, the predominant **As** species is the neutral **As(III)** arsenious acid (H₃AsO₃; pK_a = 9.29), and adsorption is less dependent on pH (Pierce and Moore 1982). Other variables affecting **As** removal efficiencies include the **As**/Fe ratio, ionic strength, and the presence of competing ions in solution.

A pilot scale **As** removal plant has been constructed at the Wairakei Geothermal Power Station to treat spent bore water by ferric flocculation. However, the HFO adsorption

of **As(III)** and **As(V)** from Wairakei geothermal bore water has been shown to be less efficient than expected when compared to adsorption from a 0.1M NaNO₃ electrolyte solution (Webster and Webster 1995). Furthermore, the observed inhibition of **As** adsorption from bore water was not predicted by the MINTEQA2 geochemical speciation model compiled by Allison et al. (1991: MINTEQA2 calculates the degree of metal adsorption using a diffuse layer adsorption model and experimentally-derived surface complexation constants). In fact, significant enhancement of **As(V)** adsorption was predicted above pH 8 by MINTEQA2, but inhibition was observed. One or more of the bore water components inhibited **As** adsorption onto HFO, and the mechanism appeared to involve solution or surface reactions which were not included in MINTEQA2's thermodynamic data base. This paper reports the results of experiments undertaken to determine the effect of individual bore water components on the HFO adsorption of **As(III)** and **As(V)** from 0.1M NaNO₃. Mechanisms for the inhibition of **As** adsorption from geothermal bore water, and the ability of MINTEQA2 to model this system, are examined.

2.0 METHODS

The HFO suspension was synthesised by rapidly raising the pH of a 0.1M NaNO₃ solution containing 1 × 10⁻³ M Fe(NO₃)₃ · 9H₂O from 2.0 to 7.0 and ageing the resulting suspension for 24 hours prior to adsorption experiments. For adsorption experiments in Wairakei bore water the 0.1M NaNO₃ solution was removed from above the settled HFO floc and replaced with bore water taken from Flash Plant No.10 at the Wairakei Geothermal Power Station. Bore water for **As(III)** adsorption experiments was used

between 1 and 3 weeks after sampling, during which time the **As** remained stable as **As(III)**. For **As(V)** adsorption experiments 5 mL of 30% H_2O_2 were added per 1L of bore water to oxidise the **As(III)** to **As(V)**. Although water treatment involves HFO precipitation *in situ*, a preformed and aged HFO was used in this work as the surface properties have been well characterised. The removal of **As** with preformed HFO and *in situ* HFO precipitation involve the same adsorption process (Fuller et al. 1993).

Adsorption experiments using synthetic solutions containing individual bore water components were prepared using the desired amount of **As** ($5.3 \times 10^{-5} \text{m}$) and adding one, or more, bore water component(s) to the HFO suspension in 0.1M NaNO_3 . Arsenic adsorption from 0.1M NaNO_3 was measured in the presence of the following bore water components: Cl^- ($6.2 \times 10^{-2} \text{m}$); SO_4^{2-} ($4.3 \times 10^{-3} \text{m}$); K^+ ($5.3 \times 10^{-3} \text{m}$); Ca^{2+} ($2.6 \times 10^{-4} \text{m}$); H_3BO_3 ($2.7 \times 10^{-3} \text{m}$); $\text{CO}_3^{2-}/\text{HCO}_3^-$ ($1.1 \times 10^{-3} \text{m}$); and H_4SiO_4 ($1.8 \times 10^{-3} \text{m}$ or $2.0 \times 10^{-3} \text{m}$). The concentrations of components used were those of Wairakei bore water as given in Ellis and Mahon (1977). Ionic species were added as the Na^+ or NO_3^- salts, H_3BO_3 was added directly and H_4SiO_4 was added as a sodium silicate solution.

Initial experiments were performed in a 1L 3 neck glass vessel on a magnetic stirrer at room temperature. The suspension pH was raised to 12 and then lowered sequentially in steps of 1-1.5 pH units with HNO_3 . The pH was remeasured and the suspension sampled 30 minutes after each pH adjustment. The sample was filtered (0.45 μm membrane) and the filtrate analysed for **As**. A 30 minute reaction time was chosen because it was similar to the time between floc formation and phase separation at the Wairakei pilot plant. Subsequent experiments determined equilibrium As adsorption from both bore

water and 0.1M NaNO_3 , with and without H_4SiO_4 . The suspension was prepared as described above and experiments were performed in HDPE bottles agitated on a side to side shaker at 25°C .

Samples were analysed for total inorganic **As** by Hydride Generation Atomic Adsorption Spectrophotometry (HGAAS) as described by Aggett and Aspell (1976). Selected samples were also analysed for **As(III)** by HGAAS on a sample buffered at pH 6 with 1M citrate buffer. This demonstrated that **As(III)** oxidation was not occurring during the **As(III)** experiments. Total silica was measured by AAS using a $\text{N}_2\text{O}/\text{C}_2\text{H}_2$ flame after adding 1mL of 1M NaOH and 10,000ppm EDTA per 10 mL sample. Molybdate-reactive silica was measured spectroscopically by the method of Iler (1979). Colour development in both bore water and sodium silicate solutions was complete within 90s and therefore all molybdate reactive silica was considered to be mono-silicic acid (H_4SiO_4).

3.0 RESULTS

The results from the 30 minute sequential experiments are described in this section, whereas the results for equilibrium experiments are given in Section 4.0 in relation to modelling **As** adsorption. The HFO adsorption of **As(III)** and **As(V)** from 0.1M NaNO_3 was not significantly affected by Cl^- , H_3BO_3 , K^+ , or $\text{CO}_3^{2-}/\text{HCO}_3^-$ at concentrations typical of Wairakei bore water. Sulfate inhibited the adsorption of **As(III)** by 5 to 10% between pH 5 and 3, but did not significantly affect **As(V)** adsorption. The bore water components having the most significant effect on **As** adsorption were H_4SiO_4 and Ca^{2+} .

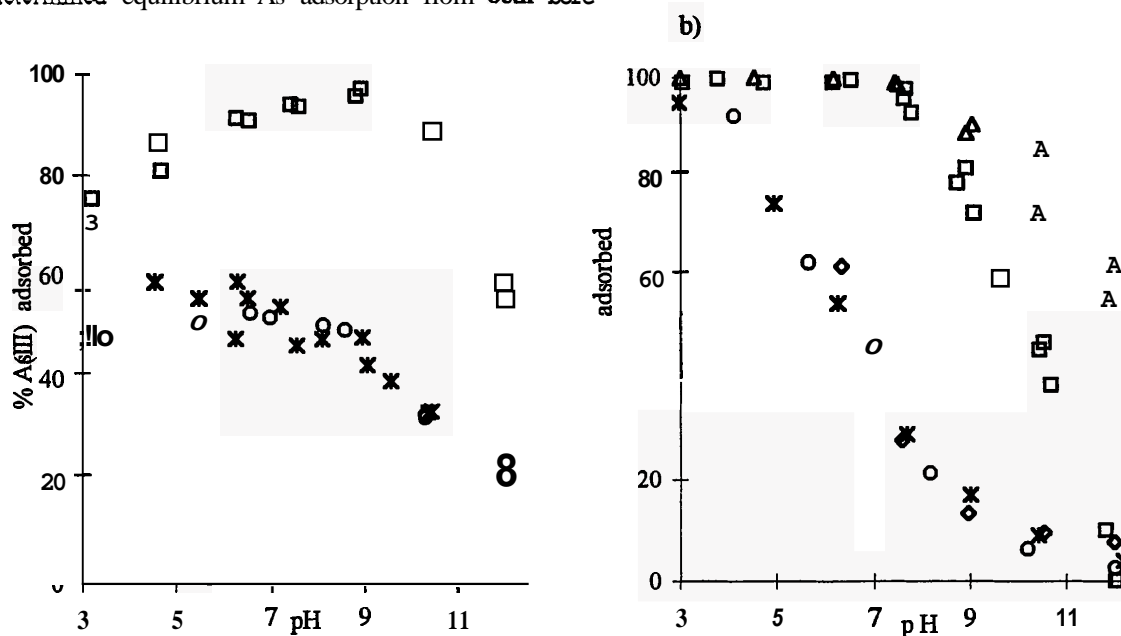


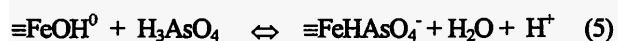
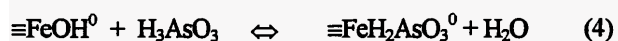
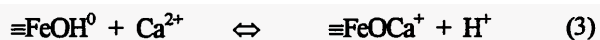
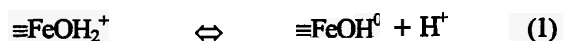
Figure 1. The adsorption of **As(III)** (a) and **As(V)** (b) from bore water compared to adsorption from 0.1M NaNO_3 , and from 0.1M NaNO_3 with H_4SiO_4 and/or Ca^{2+} . Adsorption curves shown are as follows: $5.3 \times 10^{-5} \text{m}$ **As** from 0.1M NaNO_3 (\square), $5.3 \times 10^{-5} \text{m}$ **As** from 0.1M NaNO_3 with $2.0 \times 10^{-3} \text{m}$ H_4SiO_4 (\circ), $4.7 \times 10^{-5} \text{m}$ **As** from bore water (*), $5.3 \times 10^{-5} \text{m}$ **As(V)** from 0.1M NaNO_3 with $2.6 \times 10^{-4} \text{m}$ Ca^{2+} (Δ), $5.3 \times 10^{-5} \text{m}$ **As(V)** from 0.1M NaNO_3 with $2.0 \times 10^{-3} \text{m}$ H_4SiO_4 and $2.6 \times 10^{-4} \text{m}$ Ca^{2+} (\diamond).

When Wairakei geothermal bore water is cooled, H_4SiO_4 polymerises to form an amorphous silica colloid ($\text{SiO}_{2(\text{am})}$) which has a solubility of $1.94 \times 10^{-3} \text{ m}$ at 25°C . After storing bore water at room temperature for 1 week the H_4SiO_4 concentration was stable at $2.0 \times 10^{-3} \text{ m}$, compared to the total SiO_2 concentration of $8.3 \times 10^{-3} \text{ m}$. In contrast, sodium silicate added to 0.1 m NaNO_3 at the start of As adsorption experiments was initially all present as H_4SiO_4 . The adsorption of As(III) and As(V) from 0.1 m NaNO_3 to which $2.0 \times 10^{-3} \text{ m}$ sodium silicate was added was almost identical to that observed from bore water (Figures 1(a) and 1(b)). In addition to the effect of H_4SiO_4 , the adsorption of As(V) from 0.1 m NaNO_3 at $\text{pH} > 8$ was significantly enhanced in the presence of $2.6 \times 10^{-4} \text{ m Ca}^{2+}$, although As(V) precipitation or co-precipitation with Ca^{2+} minerals was not observed in the absence of HFO. The Ca^{2+} enhancement of As(V) adsorption was not observed from bore water or from 0.1 m NaNO_3 with $2.6 \times 10^{-4} \text{ m Ca}^{2+}$ and $2.0 \times 10^{-3} \text{ m H}_4\text{SiO}_4$.

4.0 DISCUSSION

4.1 Modelling Adsorption

The surface complexation model considers adsorption as surface complex formation between sorbing species and hydroxylated surface metal sites, $\equiv\text{FeOH}^0$ (Dzombak and Morel 1990). Surface sites are considered to be amphoteric (Equations 1 and 2) and cation adsorption to be co-ordination by ionised surface hydroxyl groups (Equation 3). Oxy-anion and oxy-acid adsorption is considered as the exchange of surface hydroxyl groups with the sorbing species (Equations 4 and 5). The degree of protonation of these surface species is dependent on pH and is considered to parallel that of solution species. The extent of adsorption reactions depends upon the chemical free energy of adsorption, considered to be an intrinsic constant K^{INT} , and the coulombic free energy of adsorption, a variable term dependent on surface charge.



4.2 Adsorption of H_4SiO_4

The MINTEQA2 HFO adsorption data base did not include H_4SiO_4 binding constants due to the absence of data at the time of compilation. Therefore MINTEQA2 was not able to predict inhibition of As adsorption from bore water. The interaction between H_4SiO_4 and the HFO surface is considered to involve two processes depending on the adsorption density $\Gamma_{\text{H}_4\text{SiO}_4}$ (ie. the solid phase Si/Fe ratio; Herbillon and Tran Vinh An 1969).

The number of HFO surface sites available for adsorption is considered to be 0.2 mol per mol Fe, and when $\Gamma_{\text{H}_4\text{SiO}_4}$ is less than ca. 0.2, H_4SiO_4 is considered to adsorb at HFO surface sites in the same way as other oxy-acids, for example H_3AsO_3 in Eq. 4. This adsorption has been successfully described by the diffuse layer model for $\Gamma_{\text{H}_4\text{SiO}_4}$ of ca. 0.05, between pH 4 and 6, with an intrinsic adsorption constant $\log K_1^{\text{INT}}_{\text{H}_4\text{SiO}_4}$ of 3.62 (Hansen et al. 1994).

At $\Gamma_{\text{H}_4\text{SiO}_4}$ greater than ca. 0.2, H_4SiO_4 is considered to polymerise as a separate silica phase on the HFO surface. This polymerisation occurs at H_4SiO_4 concentrations below saturation with respect to a $\text{SiO}_{2(\text{am})}$ bulk phase and has been identified by IR and Differential Thermal Analysis of HFO exposed to H_4SiO_4 (Herbillon and Tran Vinh An 1969). For example, the temperature of crystallisation to haematite increased from 300 to 800°C as the Si/Fe ratio increased from 0 to 0.13. However, above this ratio additional Si did not affect the temperature of haematite crystallisation and characteristic silica Si-O stretching bands in the IR spectra began to appear. The polymerisation of silica on the HFO surface decreases the HFO pH point of zero charge (PZC) from 8.0 in the absence of H_4SiO_4 to ca. 4.0 with a $\Gamma_{\text{H}_4\text{SiO}_4}$ of 0.35 (Anderson and Benjamin 1985). The PZC of pure amorphous silica is approximately 2.0 (Iler 1979).

The H_4SiO_4 adsorption constant derived by Hansen et al. (1994) was added to the MINTEQA2 data base. The predicted and observed equilibrium adsorption of $1.8 \times 10^{-3} \text{ m H}_4\text{SiO}_4$ onto HFO, from 0.1 m NaNO_3 (without As) is shown in Figure 2. Adsorption of H_4SiO_4 was slow and required between 1 and 6 days to reach equilibrium. The observed H_4SiO_4 adsorption exceeded predicted adsorption, and the $\Gamma_{\text{H}_4\text{SiO}_4}$ ranged up to 0.45. This implied that significant H_4SiO_4 polymerisation had occurred at the HFO surface and, as this polymerisation is not considered by the model, MINTEQA2 could not predict this behaviour.

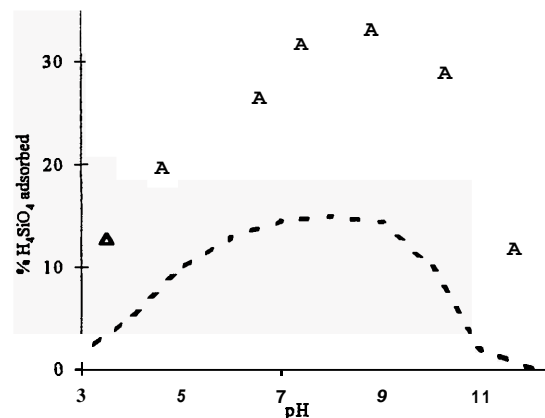


Figure 2. Comparison of the observed experimental and MINTEQA2 predicted H_4SiO_4 adsorption from 0.1 m NaNO_3 . Adsorption curves shown are MINTEQA2 predictions (---), and experimentally determined adsorption of $1.8 \times 10^{-3} \text{ m H}_4\text{SiO}_4$ (A).

4.3 Arsenic Adsorption in the Presence of H_4SiO_4

The predicted and observed equilibrium adsorption of **As(III)** and **As(V)** from bore water, and from 0.1m NaNO_3 with and without 2.0×10^{-3} m H_4SiO_4 , are given in Figures 3(a) and (b) respectively. Adsorption of **As(III)** reached equilibrium within **ca.** 24 hours, whereas adsorption of **As(V)** was more rapid, especially at low pH where equilibrium was reached in less than 1 hr, even in the presence of H_4SiO_4 . In view of the slow adsorption kinetics for H_4SiO_4 adsorption, the reason for **this** is unclear. The extent of **As(III)** and **As(V)** adsorption from bore water was almost identical to adsorption from 0.1m NaNO_3 with 1.8×10^{-3} m H_4SiO_4 .

Without alteration to the **HFO** adsorption data base, MINTEQA2 predicts **As(III)** adsorption from bore water to be similar to that from 0.1m NaNO_3 . Even when $\log K_1^{\text{NT}}_{\text{H}_4\text{SiO}_4}$ is included in MINTEQA2 the predicted **As(III)** adsorption from bore water is only **ca.** 10% less than that from 0.1m NaNO_3 , whereas the observed inhibition was between 30 and 40%. MINTEQA2's underestimation of the inhibitory effect of H_4SiO_4 on **As(III)** adsorption may again be due to its failure to take account of surface H_4SiO_4 polymerisation, which may affect **As(III)** adsorption.

MINTEQA2 under-predicted **As(V)** adsorption from 0.1m NaNO_3 , and predicted enhanced **As(V)** adsorption from bore water at $\text{pH} > 8$. **This** predicted enhancement of **As(V)** adsorption was due to the effect of Ca^{2+} adsorption on the modelled **HFO** surface charge.

From Figure 1(b) it can be seen that Ca^{2+} did enhance **As(V)** adsorption at $\text{pH} > 8$, but not from bore water nor from 0.1m NaNO_3 with 2.6×10^{-4} m Ca^{2+} which also contained 2.0×10^{-3} m H_4SiO_4 . When $\log K_1^{\text{NT}}_{\text{H}_4\text{SiO}_4}$ was added to MINTEQA2 the agreement of predicted and observed **As(V)** adsorption from bore water at $\text{pH} < 8$ was good, but possibly coincidental, due to the underestimation of both **As(V)** adsorption from 0.1m NaNO_3 and the effect of H_4SiO_4 on **As(V)** adsorption. The predicted **As(V)** adsorption from bore water was still enhanced at $\text{pH} > 8$ when MINTEQA2 included $\log K_1^{\text{NT}}_{\text{H}_4\text{SiO}_4}$, though **this** was not observed.

There are several possible reasons why the Ca^{2+} enhancement of **As(V)** adsorption was not observed from system with H_4SiO_4 . In bore water both the precipitation of CaCO_3 at $\text{pH} > 10$ and/or the interaction between Ca^{2+} and colloidal silica may prevent Ca^{2+} enhancing **As(V)** adsorption. However, neither a CaCO_3 precipitate nor colloidal silica were present in the 0.1m NaNO_3 solution with Ca^{2+} and H_4SiO_4 (Figure 1b). In **this** system the silica phase formed by the polymerisation of H_4SiO_4 on the **HFO** surface, being more negatively charged than the **HFO**, could either offset the effect that Ca^{2+} adsorption had on **HFO** surface charge and/or attract Ca^{2+} more strongly than the **HFO** phase. In addition, although no precipitation was observed from 0.1m NaNO_3 solutions with Ca^{2+} and H_4SiO_4 in the absence of **HFO**, there are several calcium silicate minerals that may form as an indiscernible colloid which could have removed Ca^{2+} from **this** solution.

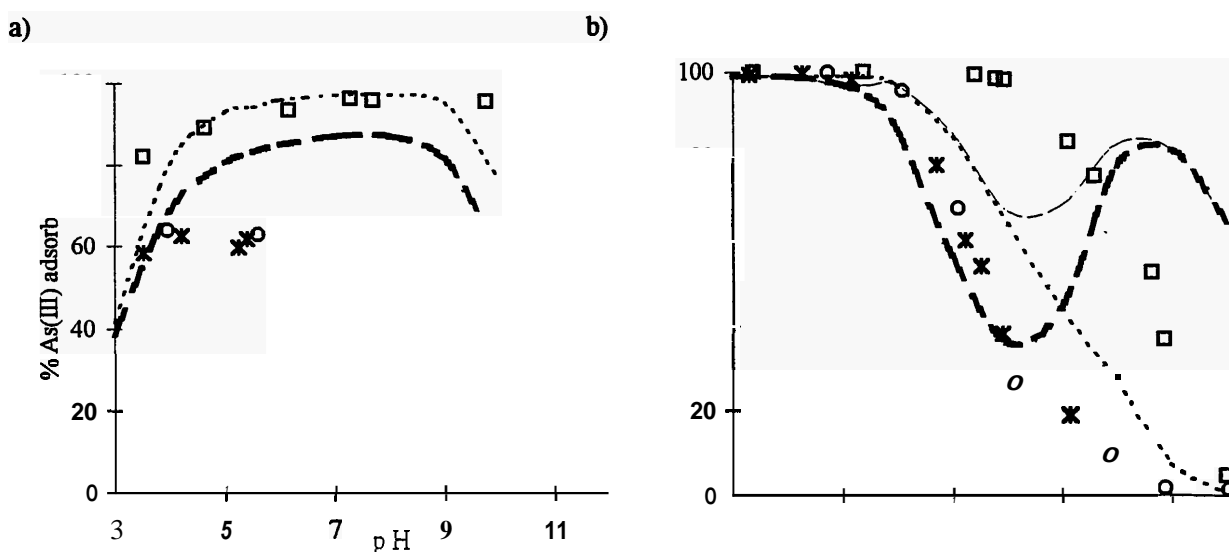


Figure 3. Comparison of the experimental and MINTEQA2 predicted **As(III)** (a) and **As(V)** (b) adsorption from bore water, and from 0.1m NaNO_3 with and without H_4SiO_4 . Adsorption curves are shown as follows; 5.3×10^{-5} m **As** from 0.1m NaNO_3 (O), 5.3×10^{-5} m **As** from 0.1m NaNO_3 with 2.0×10^{-3} m H_4SiO_4 (o), 4.7×10^{-5} m **As** from bore water (*), MINTEQA2 predicted adsorption for 5.3×10^{-5} m **As** from 0.1m NaNO_3 (---), MINTEQA2 (without K_1 for H_4SiO_4 adsorption) predicted adsorption for 4.7×10^{-5} m **As(V)** from bore water (— →) and MINTEQA2 (altered to include a K_1 for H_4SiO_4 adsorption) predicted adsorption for 4.7×10^{-5} m **As** from bore water (- - -).

5.0 CONCLUSION

Flocculation **with HFO** can be an effective water treatment process to remove As from geothermal bore water. Because **the** adsorption of As(III) and As(V) from bore water is inhibited by the high concentrations of H_4SiO_4 found in bore water, efficient **As** removal can only be achieved at low pH and with the As(V) oxidation state. The bore water H_4SiO_4 appears to inhibit As adsorption by competition for adsorption sites and **by** polymerising on the HFO surface. The ability of MINTEQA2 to predict **As** adsorption from bore water is improved by including the K_1 for H_4SiO_4 adsorption derived by Hansen et al. (1994). However, the effect of H_4SiO_4 polymerisation is not considered **by** MINTEQA2, and the $\text{Ca}^{2+}/\text{H}_4\text{SiO}_4/\text{HFO}$ interactions **are** therefore incorrectly modelled.

6.0 ACKNOWLEDGMENTS

This work was undertaken **as** an MSc thesis **with** the School of Environmental and Marine Sciences at the University of Auckland. We would like to acknowledge the help and collaboration of **Mr** Lew Bacon and **Mr** Jo Jordan (CONTACT Geothermal Energy, Wairakei Power Station), Dr Kevin Brown (IGNS) and Kerry Webster (ESR).

7.0 REFERENCES

- Aggett, J. and Aspell, A. C. (1976). The determination of arsenic (III) and total arsenic **by** atomic-adsorption spectroscopy. *The Analyst*, Vol. 101, 341 - 347.
- Aggett, J. and Aspell, A. C. (1978). *Release of Arsenic From Geothermal Sources*. Report No. 35 New Zealand Energy and Development Committee (NZERDC), Wellington.
- Allison, J. D., Brown, D. S. and Novo-Gradac, K. J. (1991). *MINTEQA2/PRODEFA2, A Geochemical Assessment Model for Environmental Systems: Version 3.0 User's Manual*. EPA/600/3-91/021, USEPA, Athens, Georgia.
- Anderson, P. R. and Benjamin, M. M. (1985). Effects of silicon on the crystallisation and adsorption properties of ferric oxides. *Environ. Sci. Technol.*, Vol 19, 1048 - 1053.
- Davies, J. E., Alders, W. W. and Deely, J. M. (1994). *Arsenic in Drinking Water: Investigation of At-Risk Supplies*. Report Prepared **by** ESR Health for the Ministry of Health, Wellington.
- Dzombak, D. A. and Morel F. M. M. (1990). *Surface Complexation Modelling; Hydrous Ferric Oxide*, John Wiley & Sons, New York.
- Ellis, A. J. & Mahon, W. A. J. (1977). *Chemistry and Geothermal Systems*, Academic Press, New York.
- Fuller, C., Davis, J. A. and Waychunas, G. A. (1993). Surface chemistry of ferrihydrite: Part 2. Kinetics of arsenate adsorption and co-precipitation. *Geochimica et Cosmochimica Acta*, Vol 57, 2271 - 2282.
- Hansen, H. C. B., Wethe, T. P., Raulund-Rasmussen K. and Borggaard, O. K. (1994). Stability **constants** for silicate adsorbed to ferrihydrite. *Clay Minerals*, Vol 29, 341-350.
- Herbillon, A. J. and Tran Vinh An, J., (1969). Heterogeneity in silicon-iron mixed hydroxides. *Journal of Soil Science*, Vol 20, No. 2, 223 - 235.
- Iler, R. K., (1979). *The Chemistry of Silica - Solubility, Polymerisation, Colloid and Surface Properties, and Biochemistry*. John Wiley & Sons, New York.
- Peng, F. F. and Di, P. (1994). Removal of arsenic **from** aqueous solution **by** adsorbing colloid flotation. *Ind. Eng. Chem. Res.*, Vol 33, 922 - 928.
- Pierce, M. T. and Moore, C. B. (1982). Adsorption of arsenite and arsenate on amorphous iron hydroxide. *Water Res.*, Vol 16, 1247 - 1253.
- Webster, J. G. and Webster, K. S. (1995). Arsenic adsorption **from** geothermal water. *Proceedings of 16th Annual PNOC Geothermal Conference*, Manila, Philippines, 35 - 42.
- World Health Organisation (1993). *Guidelines for Drinking Water Quality, 2nd Ed, Volume I Recommendations*, World Health Organisation, Geneva.